Experimental and numerical analysis of hydrogen interaction with plastic strain in a high strength steel

Flavien Vucko, Cédric Bosch, David Delafosse

To cite this version:

Flavien Vucko, Cédric Bosch, David Delafosse. Experimental and numerical analysis of hydrogen interaction with plastic strain in a high strength steel. European Corrosion Congress - Eurocorr 2012, Sep 2012, Istanbul, Turkey. Paper 1223. emse-01063843

HAL Id: emse-01063843
https://hal-emse.ccsd.cnrs.fr/emse-01063843
Submitted on 14 Sep 2014

Experimental and numerical analysis of hydrogen interaction with plastic strain in a high strength steel

F. Vucko[1]*, C. Bosch, D. Delafosse, Ecole Nationale Supérieure des Mines, SMS-EMSE, CNRS: UMR 5146, LCG, 158 cours Fauriel, 42023 Saint-Etienne, France*

Summary

Cyclic loading tests were performed on micro-notched samples of high-strength steel S690QT in air and under cathodic polarisation in a saline solution. These specimens were modelled and their behaviour simulated by finite elements calculations with a combined nonlinear isotropic-kinematic hardening constitutive law. This model can simulate cyclic softening and ratcheting effect of the high-strength steel. Stress and strain fields in the vicinity of the notch-tip were calculated. Results show that a strong dependence of the crack initiation with plastic strain accumulation. Hydrogen assisted cracking mechanism is discussed based on arrangements of dislocations structures.

1 Introduction

The interest in the use of high-strength steels as structural materials is both environmental and economic since it allows lightening the weight of structures. Nevertheless, these materials are very sensitive to hydrogen effect which could be responsible of severe damages in the presence of hydrogen sources. Many studies have shown that this sensitivity increases with the mechanical strength of steels [1]. Furthermore in hydrogenating conditions, tensile properties and fatigue behaviour are modified [2-5]. The sensitivity to surface defects is also affected by hydrogen [6]. Indeed both effect of hydrostatic stress gradient on the chemical potential of hydrogen and localization of plastic strain at defect-tips promote the increase of hydrogen content and hydrogen-plasticity interactions.

In this paper, we presented an experimental method and simulation procedure to investigate and quantify the role of plastic strain, stress and hydrogen trapping on the mechanisms of initiation and propagation of cracking of quenched and tempered martensitic steel in a hydrogenating environment. Mechanical tests at constant and cyclic loading were performed on micro-notched specimens under cathodic polarization in de-aerated saline solution. The strain hardening (or softening) rate at notch-tip was fitted by controlling the maximum stress, the stress ratio and the number of cycles applied. Specimens were instrumented to monitor crack initiation and crack growth rate with a DCPD (Direct Current Potential Drop) method. Added to these tests, numerical simulations on finite elements code ZeBuLon have modelled the mechanical behaviour of the steel at the micro-notch root. Stress and strain fields in the vicinity of notch-tip have been determined.

This paper is divided in four parts. In the first one, we present the material and its mechanical behaviour. The second part deals with the procedure for hydrogen assisted cracking (HAC) tests, and explains the role of micro-notch on specimens. Then, the combined nonlinear isotropic-kinematic hardening material constitutive law

---

[1] Corresponding author

Tel.: +33 4 77499775; fax: +33 4 77420157

E-mail address: vucko@emse.fr

used to model the behaviour of the steel is presented in detail. Finally, experimental results on crack initiation are analysed and discussed based on FE calculations of stress and plastic strain fields at notch-tip.

2 Material and mechanical behaviour

The material of the study is a high-strength steel S690 (ASTM A514). It presents a tempered martensitic microstructure (figure 1) consisting of laths of 1 to 2 µm wide and few cementite along lath boundaries. The duration and temperature of the tempering were two hours at 550℃. Prior austenite grain size is ranging from 10 to 20µm. No retained austenite has been detected by X-Ray analysis.

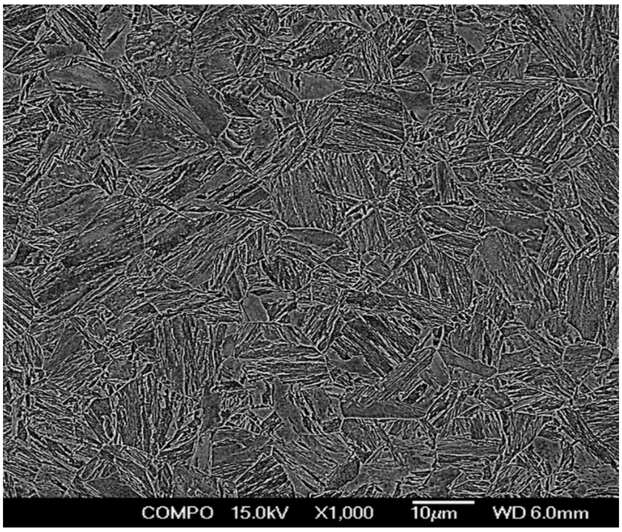

Fig. 1: SEM observation of the microstructure of S690QT steel

Yield stress, ultimate tensile stress and elongation are respectively 726MPa, 900MPa and 21.8%. This steel presents a typical cyclic softening under fatigue solicitations as shown on figure 2a. Softening can be divided in two stages (figure 2b): a strong softening stage up to a cumulative plastic strain value of about 2 followed by a weak softening conducting to a pseudo stability stage.

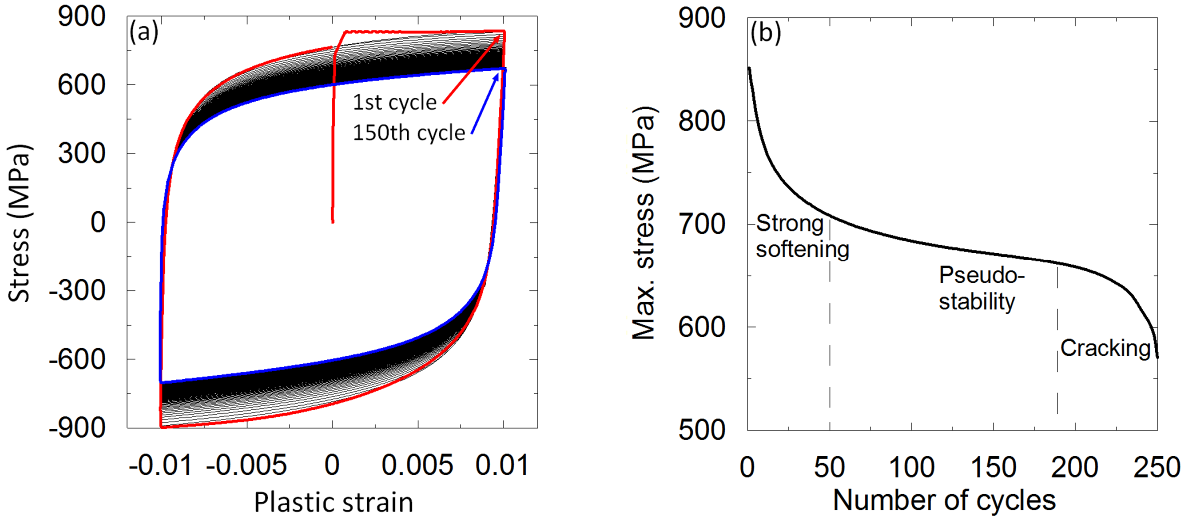

Fig. 2: (a) Hysteresis loops under fatigue solicitation (plastic strain amplitude of 2% at plastic strain rate of 5×10^{-4} s^{-1}), (b) Maximal stress vs. number of cycles

Cyclic softening is controlled by the microstructure of the material [7-9]. During cyclic loading, density of dislocations decreases inside subgrains and the size of these subgrains can increases with plastic strain accumulation.

3 Hydrogen Assisted cracking tests

1. Micro-notched specimens

HAC tests have been performed on micro-notched specimens. Notches were machined with a precision saw wire in order to avoid strain hardening. Notch radius is 40µm and depth is about 300µm. This specific geometry of specimens has some interesting advantages. First of all, a notch provides a plastic zone that might concentrate hydrogen-plastic strain interactions. As a result, a single crack initiates on the notch-tip and so cracking can be monitored by a DCPD method to determined crack initiation and brittle crack growth rate, as used in this study (see figure 3 as an example of an in situ crack monitoring). Moreover, complex but controlled stress and strain fields can be developed on the notch-tip with simple loadings. Thanks to tensile-tensile fatigue tests with different load ratios R, plastic strain can be accumulated on the notch-tip (see figure 4).

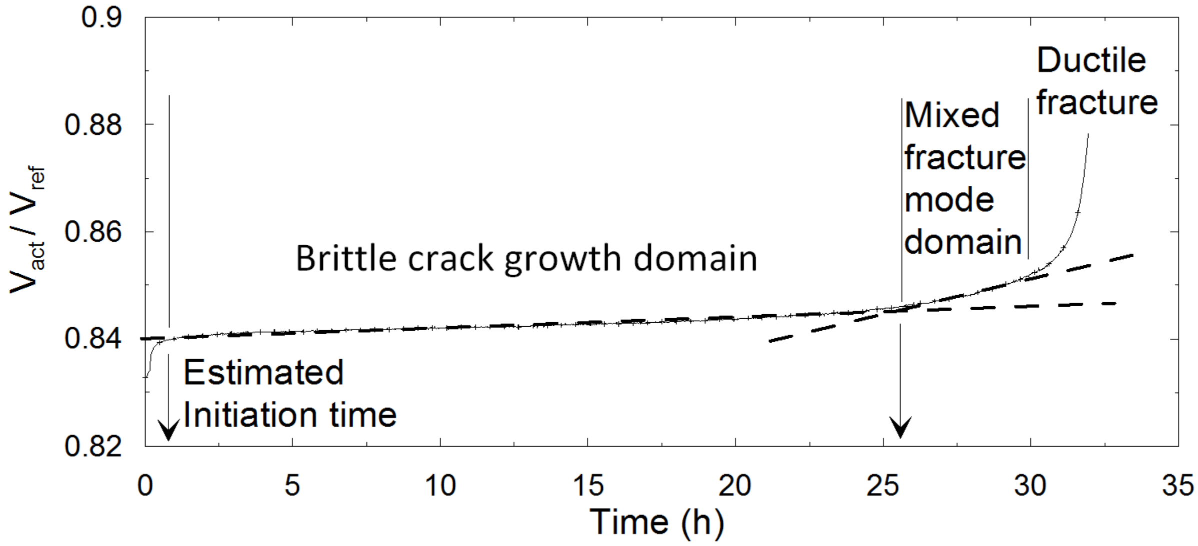

Fig. 3: In situ monitoring of cracking by DCPD method

No direct measurement of the level of stress and strain on the notch-tip can be made. Some simulations have to be developed to estimate these parameters. This modelling is discussed in the next part.

2. Tests procedure

Specimens are hydrogen charged by cathodic polarization in 30g.L^{-1} NaCl solution at -1200mV/SCE. The solution was de-aerated and buffered at pH 4.5 by bubbling in a gas mixture of nitrogen with 7% of carbon dioxide. The charging process was applied 12 hours before the mechanical loading and maintained throughout tests.

Levels of plastic strain and strain softening are controlled using tensile-tensile tests as discussed earlier and represented on figure 4. The maximal stress value varies from 88 to 95% of the yield strength and load ratios from 0.5 to 0.8. Frequency has been chosen equal to 10^{-3}Hz. These tests lead to a gradual cyclic softening where cumulated plastic strain at micro-notch-tip depends on load ratio and number of cycles.

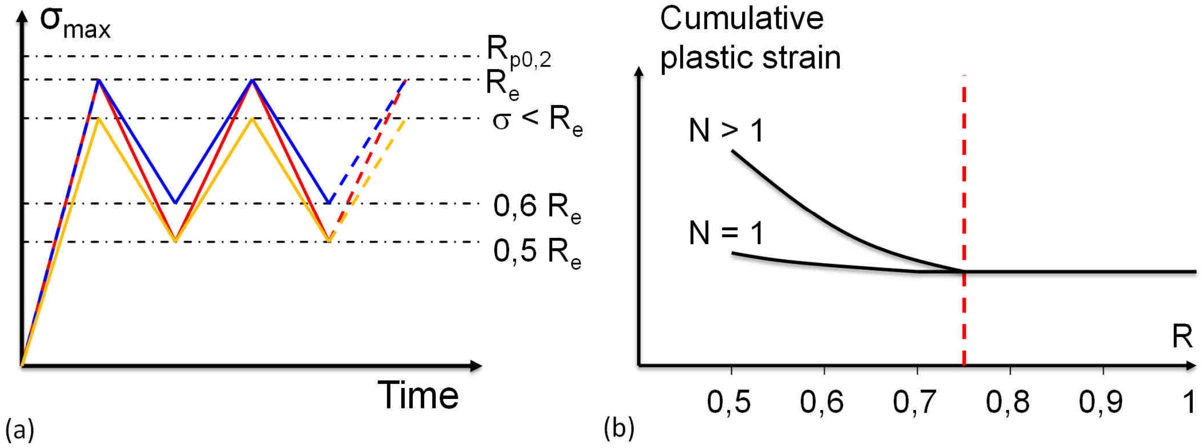

Figure 4: (a) Tensile-tensile fatigue solicitations, (b) notch-tip response to tensile-tensile solicitations (experimental and simulation results)

4 Material modelling

Behaviour modelling

Many constitutive laws have been developed to model mechanical behaviour of metals. Isotropic and kinematic laws derive from thermodynamical formulation [10, 11]. Combined laws were then developed [12, 13] to allow description of phenomena as Bauschinger effect, ratcheting effect and cyclic softening/hardening which occur around the notch. This kind of law is necessary to describe accurately the behaviour of the steel.

Two hardening variables are used to describe this model. The backstress tensor ***X*** is the kinematic variable and the thermodynamic force *R* is the scalar isotropic variable. From a mechanical point of view, kinematic hardening is the displacement of the centre of the yield surface and isotropic hardening is the expansion/contraction of this surface.

Their evolution equations are:

$$\underline{\underline{\dot{X}}} = \sum_i \underline{\underline{\dot{X}}}_i \text{ with } \underline{\underline{\dot{X}}}_i = c_i \dot{\varepsilon}^p - \gamma_i \underline{\underline{X}}_i \dot{p} \qquad \text{Eq.1}$$

$$\dot{R} = b(Q-R)dp \qquad \text{Eq.2}$$

where c_i, γ_i, b, Q are material dependant constants. One way to take into account the isotropic hardening is to introduce a function of the cumulative plastic strain $c_i(p)$ in the kinematic variable ***X***:

$$\underline{\underline{\dot{X}}}_i = c_i(p)\dot{\varepsilon}^p - \gamma_i \underline{\underline{X}}_i \dot{p} \text{ with } c_i(p) = \frac{C_i}{\sigma^0(p)} \qquad \text{Eq.3}$$

C_i is a material dependant constant and $\sigma^0(p)$ is an exponential law which modelled the isotropic hardening:

$$\sigma^0(p) = \sigma_y + Q(1-e^{-bp}) \qquad \text{Eq.4}$$

where σ_y is the strain-independent yield stress; Q is the asymptotic value when the saturated stage is reached; b is the rate at which the stage is attained.

This model has been implemented in the finite elements code ZeBuLon.

Calibration and validation of the model

Model parameters identification is based on low cycle fatigue tests at different plastic strain amplitude (from 0.4 to 4%) and at constant strain rate (5×10^{-4} s^{-1}). Using graphical optimization, the model has been fitted to experimental data. An initial work hardened state has been considered through an initial backstress tensor.

A simulated low cycle fatigue test at 1% of plastic strain amplitude is presented on figure 5a and results are compared to experimental data on figure 5b. The model follows quite well the cyclic softening of the material and shapes of hysteresis loops are in accordance with experimental observations.

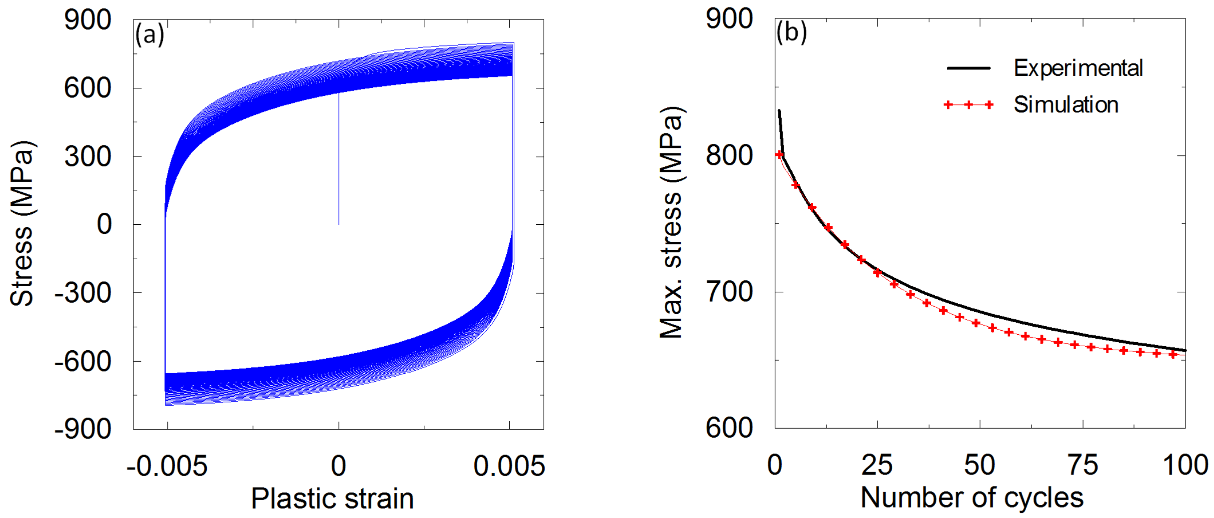

Fig. 5: (a) Simulated hysteresis loops for plastic strain amplitude of 1%, (b) Maximal stress vs. number of cycles from simulation and experimental data.

Simulation of initiation stage of cracking tests

Tensile-tensile fatigue tests on notched specimens have been simulated on FE code ZeBuLon. The mesh around the notch and the integration point used for stress and strain calculations is presented on figure 6a.

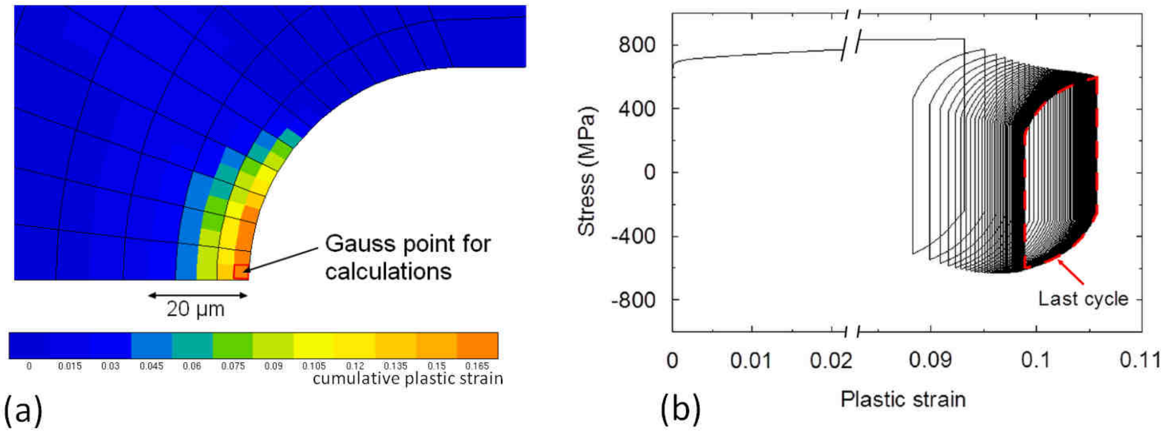

Fig. 6: (a) Mesh around the notch, (b) notch-tip response to tensile-tensile solicitations (simulation for R=0.5 and σ_{max}=88%YS)

Stress vs. plastic strain on the notch-tip is plotted on figure 6b. The notch exhibits an asymmetric loading during the first cycles which leads to a ratcheting effect on the plastic strain. Accumulation of plastic strain is responsible of a strong softening till a saturation stage. The softening is related to relaxation of the mean stress down to zero and intrinsic softening of the material with cumulative plastic strain.

5 Analysis of the notch-tip

Crack initiation times obtained with DCPD method are reported on figure 7 as a function of load ratios. The maximum initial stresses on the notch-tip, $\sigma_{notch\text{-}tip}$, calculated by FE are also reported on the graph. They are ranged from 831 to 843 MPa.

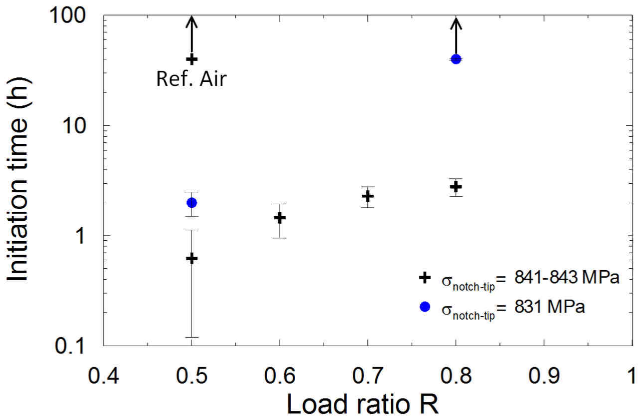

Fig. 7: Initiation times of tensile-tensile fatigue tests

The crack initiation time clearly depends on stress and load ratio applied. For a given maximum stress applied, the greater is the load ratio the longer is the initiation time. While for a given load ratio, increasing applied stress decreases the initiation time. For the higher load ratio (R=0.8), no crack initiation occurred at the lowest $\sigma_{notch\text{-}tip}$. Similarly, test performed in air in the harshest mechanical conditions has no crack.

Investigations with the FE model show that for a given maximum stress applied, the greater is the load ratio the smaller is the swept amplitude of stress and plastic strain at each cycle (see figure 8 for plastic strain). Consequently, the cumulative plastic strain is more important for low load ratios. Increasing load ratio up to 0.8 reduces the strain amplitude to zero and no more plastic strain occurs after the first quarter of cycle.

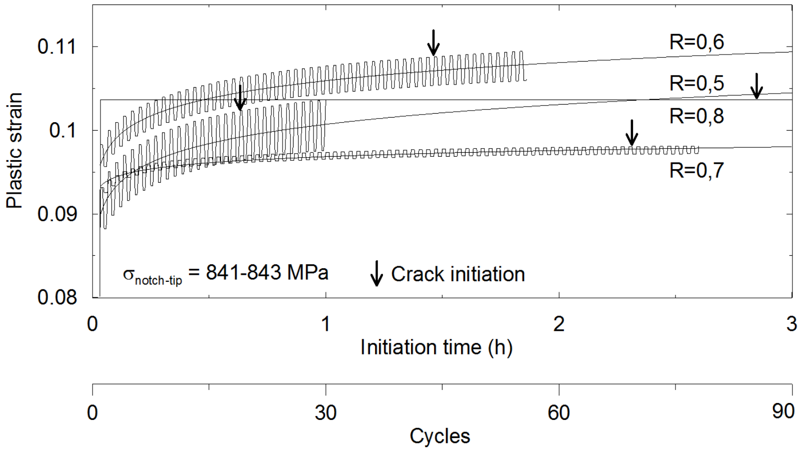

Fig. 8: Plastic strain vs. number of cycles at different load ratios

The evolution of the maximum stress at the notch-tip during first cycles is represented in figure 9. For load ratios smaller than 0.8, cyclic softening occurs in three stages: an initial strong softening with a rate identical for all the conditions of loading explored; a second stage where the rate decreases; and a saturation stage with a small and constant rate of softening.

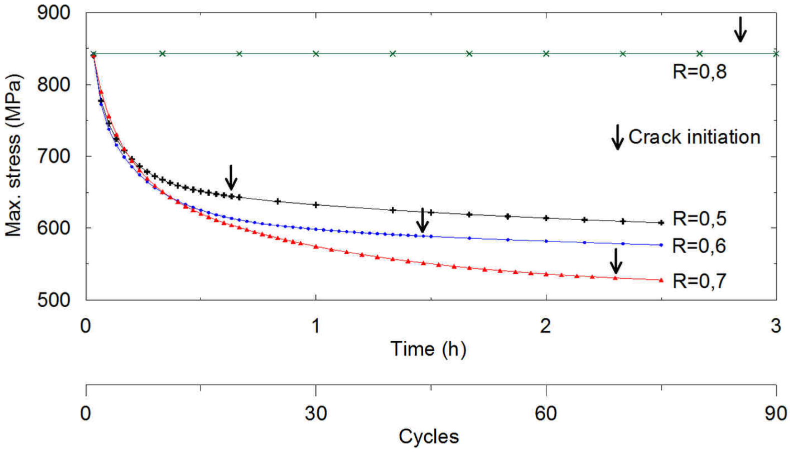

Figure 9: Evolution of maximum stress at different load ratios

At R=0.5, the saturation stage begins at about 15 cycles, much earlier than at 0.6 and 0.7. It indicates that increasing the stress amplitude, and so the plastic strain amplitude, contributes to reach more quickly the saturation stage. Plastic strain accommodation to the mechanical solicitation is faster. The maximum stress at notch-tip on the saturation stage depends on the level of initial mean stress. At high R-ratios, the mean stress is important which induces a high cyclic softening. For smaller R-ratios, the initial mean stress is lower so cyclic softening is weaker.

Crack initiations (see arrows on graph figure 9) occur at the beginning of the saturation stage, so crack initiation times seem to be shorter as maximum stress at notch-tip is high. Nevertheless, test at R=0.8 shows this is not the only factor of HAC damage.

FE calculations for tests loaded at $\sigma_{\text{notch-tip}}$ =831MPa present similar results: no accumulation of plastic strain at R=0.8 whereas plastic strain occurs at each cycle at R=0.5 (see figure 10). Compared to previous results crack initiation is delayed by a factor three at least at R=0.5 but no crack has been detected at R=0.8. In this last condition, stress applied seems to be too low to initiate a crack. Consequently HAC at R=0.5 can be attributed to plastic strain accumulation.

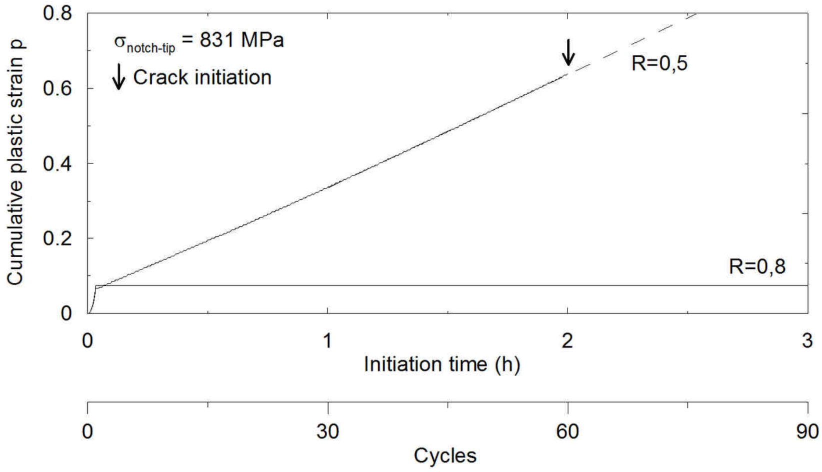

Fig. 10: Accumulation of plastic strain at lower maximum stress

All these tensile-tensile fatigue tests have shown that accumulation of plastic strain cycle by cycle is coupled with the cyclic softening of the steel at the notch-tip. Thus, while local stress decreases, cumulative plastic strain increases. Softening is associated to microstructural changes: width of martensite laths increases and dislocations are structured in cells [14]. These evolutions modify both the distribution, in a more heterogeneous manner, and the content of hydrogen at the notch-tip. Moreover, cyclic loadings during hydrogen cathodic charging increase point defect population, presumably vacancies, which enhanced the susceptibility to HAC [15].

6 Conclusion

A local approach of fracture method has been developed to investigate sensitivity to HAC of a high strength steel S690QT. Cyclic behaviour has been modelled by FE using a combined nonlinear isotropic-kinematic hardening constitutive law. Calculations of local mechanical variables were used to analyse HAC tests.

Crack initiation time depended on both cumulative plastic strain and current value of stress at notch-tip. At load ratios below 0.8, plastic strain occurred at each cycle which contributes to decrease initiation time even when local stress is decreased. Moreover, when stress is not high enough to initiate a crack, accumulation of plastic strain and modifications of microstructure associated can trigger the cracking conditions.

References

[1] Hirth JP. Effects of hydrogen on the properties of iron and steel. Metall Mater Trans A 1980; 11:861-90

[2] Brass A-M, Chêne J. Hydrogen uptake in 316L stainless steel: Consequences on the tensile properties. Corros Sci Vol 2006; 48:3222-42

[3] Hardie D, Charles EA, Lopez AH. Hydrogen embrittlement of high strength pipeline steels. Corros Sci 2006; 48:4378-85

[4] Huneau B, Mendez J. Evaluation of environmental effects on fatigue crack growth behaviour of a high strength steel in a saline solution with cathodic protection. Int J Fatigue 2006; 28:124-31

[5] Murakami Y, Matsuoka S. Effect of hydrogen on fatigue crack growth of metals. Eng Fract Mech 2010; 77:1926-40

[6] Sofronis P, McMeeking RM. Numerical analysis of hydrogen transport near a blunting crack tip. J Mech Phys Solids 1989; 37:317-50

[7] Chai HF, Laird C. Mechanisms of cyclic softening and cyclic creep in low carbon steel. Mater Sci Eng 1987; 93:159-74

[8] Fournier B, et al. Microstructural evolutions and cyclic softening of 9%Cr martensitic steels. J Nucl Mater 2009; 386-388: 71-4

[9] Giordana MF et al. Microstructure evolution during cyclic tests on EUROFER 97 at room temperature. TEM observation and modelling. Mater Sci Eng A 2012; 550:103-11

[10] Prager W. A new method of analyzing stresses and strains in work-hardening plastic solids. ASME J Appl Mech 1956; 23:493

[11] Ziegler H. A modification of Prager’s hardening rule. Quart Appl Math 1959; 17:55

[12] Armstrong PJ, Frederick CO. A mathematical representation of the multiaxial Bauschinger effect. Materials at high temperature 1966; 24:1-26

[13] Chaboche J-L. On some modifications of kinematic hardening to improve the description of ratcheting effect. Int J Plasticity 1991; 7:661-78

[14] Kim DW, Kim SS. Contribution of microstructure and slip system to cyclic softening of 9 wt.%Cr steel. Inter J Fatigue 2012; 36:24-9

[15] Nagumo M, Sekiguchi S, Hayashi H, Takai K. Enhanced susceptibility to delayed fracture in pre-fatigue martensitic steel. Mater Sci Eng A 2003; 344:86-91.